Catalysis Letters Vol. 113, Nos. 1–2, January 2007 (© 2007)
DOI: 10.1007/s10562-006-9008-2

Pre-prepared platinum nanoparticles supported on SBA-15 – preparation, pretreatment conditions and catalytic properties

Zoltan Kónya[a,*], Eva Molnar[a], G. Tasi[a], Krisztian Niesz[a,b], Gabor A. Somorjai[b] , and Imre Kiricsi[a]

[a]*Department of Applied and Environmental Chemistry, University of Szeged, Rerrich Bela ter 1, H-6720, Szeged, Hungary*
[b]*Chemistry Department, University of California, Berkeley, Berkeley, CA 94720, USA*

Received 29 September 2006; accepted 15 November 2006

The primary objective of this paper is the complete characterization of Pt/SBA-15 catalysts prepared by sonication aided impregnation. During the experiments (i) the influence of sonication applied for introducing the already prepared platinum nanoparticles into the pores of the silica support, (ii) the pressure used for preparing the tablets and/or wafers for catalytic test, (iii) the temperature of heat treatment on the structural changes of catalyst samples, (iv) the effect of platinum particle concentration, and (v) the removal of rest organic matter from the catalysts by different procedures were systematically studied. The samples were characterized by nitrogen adsorption/desorption measurements (BET), TEM, SAXS, XRD and IR. The catalytic activity of the samples was also investigated in the reaction of cyclohexene hydrogenation.

KEY WORDS: metal nanoparticles; mesoporous materials; cyclohexene hydrogenation.

1. Introduction

The preparation of a catalyst operating at high activity and selectivity wrestles with several difficulties. The mechanical and thermal stability of a catalyst is strongly influenced by the nature of the precursors and the preparation methods applied for manufacturing the catalytic matter or on the pretreatment of catalyst preceding the catalytic runs [1,2].

The general procedures for preparation of supported metal catalysts can be classified into three groups. The first consist in the impregnation of the support by the appropriate solution of metal salt followed by the decomposition of this salt and the reduction of the metal ions to form metal nanoparticles. In the second procedure generally used for support matter of ion exchange properties, such as zeolites, etc., the exchange capacity is utilized to introduce the metal ion. The third procedure is the vapor deposition in which the volatile metal compound is deposited on the support.

Recently, a novel preparation procedure has been described for the synthesis of precisely controlled (shape and size) noble metal nanoparticles containing catalyst [3]. In this process noble metal particles of known morphology are prepared and these uniformly sized nanocrystals are introduced into the pore system of the support. Mesoporous silicates, especially SBA-15 silicate were used in part of these experiments since the size of the regularly ordered pores was comparable to the measure of the platinum nanocrystals [4]. The following three basic procedures are known to incorporate pre-prepared metal nanoparticles:

(i) simple impregnation of the mesoporous silicate with colloid solution of platinum particles;
(ii) using intensive sonication to assist the introduction of metal particles mostly into the pores, since the energy of the ultrasonic waves may help to hammer the metal nanoparticles into the pores;
(iii) synthesis of the silicate around the pre-prepared platinum nanoparticles enclosure the metal nanocrystals in the channels of the mesoporous oxide.

We have reported the preparation and characterization of catalyst samples prepared by synthesis of silicate around the pre-prepared platinum particles, some characteristics of supported platinum catalysts prepared by impregnation of platinum particles on SBA-15 support. Some aspects of this preparation method can be found elsewhere [5].

Yang and his co-workers used Transmission Electron Microscopy to investigate the effect of heat treatment (25–800 °C) on the shape of supported Pt nanoparticles. They found that the particles are stable under 350–500 °C, and above 500 °C they lose their shape. The authors believe that this relatively large stability can be attributed to the interfacial mixing of platinum and SiO_2 and the negative interface energy [6].

For MCM-41, MCM-48, FSM-16 and HMS mesoporous materials the intensive research led to the determination of the factors influencing the stability of these silicates [7,8]. Several authors gave potential

*To whom correspondence should be addressed.
E-mail: konya@chem.u-szeged.hu

solution to overcome the problem of low mechanical and thermal stability of the mentioned materials that are potential catalyst supports [9,10]. Tatsumi group suggested a post synthesis treatment using silanes [11,12], while Fudala *et al.* suggested strengthening the MCM-41 structure by packing the tubes between layer silicates [13]. The most characteristic feature concluded from these papers was that up to 5–6 MPa pressure there was no detectable change in the XRD profiles and in the BET values. At higher pressure significant changes occurred. Although the thermal stability of M41S type materials (e.g. MCM-41) has been thoroughly investigated and reported, similar systematic studies are not yet available for SBA-15 supported metal catalysts.

In this paper we intend to report the characterization of catalysts prepared by sonication aided impregnation. The detailed aim of this work was to study (i) the influence of sonication applied for introducing the pre-prepared platinum nanoclusters into the pores of the silica support, and (ii) the influence of pressure and temperature of heat treatment under inert atmosphere or in vacuum on the structural changes of catalyst samples of different platinum particle concentration.

2. Experimental

2.1. Chemicals

Potassium tetrachloroplatinate (K_2PtCl_4, 99.9%, metals basis) was purchased from Alfa Aesar. Sodium polyacrylate (SPA), poly(vinylpyrrolidon) (PVP) and poly(*N*-isopropylacrylamide (NIPA) was obtained from Sigma-Aldrich. Pluronic P123 tri-block copolymer surfactant (poly(ethylene oxide)-poly(propylene oxide)-poly(ethylene oxide) –$PEO_{20}PPO_{70}PEO_{20}$) was obtained from BASF Corporation as a research sample.

2.2. Sample preparation

The preparation of platinum nanoparticles in aqueous media requires the use surface protecting compounds introduced into the platinum salt solution before the reduction step. Several organic molecules are suggested for this purpose [14–16]. In this study two different molecules, PVP (poly(vinylpyrrolidon)) and NIPA (poly(*N*-isopropylacrylamide)) were used as surface protecting agents to regulate the morphology of the platinum nanoparticles. The synthesis procedure was described elsewhere [17]. Briefly, the required amount of polymer was dissolved in distilled water. The estimated amount (to obtain 10^{-4} molar solvent) of platinum salt (K_2PtCl_4) was added while stirring. For reduction hydrogen was used. First pure nitrogen was bubbled through the solvent for 20 min followed by reduction with hydrogen for 10 min. After stopping the gas streams the vessel was closed and stored in darkness for 12 h. The shape of particles was influenced by the temperature of crystallization. The yellow colored colloidal solution of platinum nanoparticles was stored in refrigerator. The dominant shape of the particles determined by TEM was cubic.

Synthesis of SBA-15 mesoporous silicate was performed by the procedure suggested by Stucky [18]. Briefly, a solution of $PEO_{20}PPO_{70}PEO_{20}$:cc.HCl:tetraethoxysilane:water = 2:15:3.6:60 (mass ratio) was prepared, stirred for 24 h at 35 °C, and then heated at 85 °C for 1 day. The products were washed, dried and calcined at 550 °C for 12 h to remove the template. This was the starting matter for impregnation.

For samples prepared by sonication aided impregnation the procedure was as follows. The calculated amount of template free SBA-15 sample was suspended in aqueous solution of platinum nanoparticles and after closing the flask it was placed into the sonication bath (Elma Transsonic T570/H) for 10 h. When the treatment finished the solid sample was handled as for the impregnation procedure. The platinum content were 0.01–1 wt%.

For comparison a sample was prepared by a conventional impregnation of SBA-15 support with aqueous colloid solution of platinum nanoparticles synthesized in the absence of any surface protecting agents using a Rotavap system in order to homogenize the platinum distribution upon the evaporation of the solvent. The samples were dried and stored at room temperature before characterization and catalytic test.

2.3. Sample characterization

The supported platinum samples were characterized by Small Angle X-ray Scattering (SAXS) measurements. The characteristic patterns were recorded on a Bruker Nanostar U diffractometer using CuKα radiation (1.54 Å) with a sample to detector distance of 107 cm. The change in the ordering of the mesoporous silica substrate is effected by the catalyst pretreatment was determined from the characteristic peak positions and the related intensities.

For taking the TEM images a Philips CM 10 microscope was used. Small portion of samples were suspended in ethanol and a drop of this suspension was put onto the grid made from copper, dried and measured.

Adsorption of nitrogen was measured at 77 K with a Quantachrome Instruments, NOVA 2000, and the BET surface area and the pore size distribution were determined from the isotherms. Pore size distribution (PSD) curves were calculated from the adsorption branch of the isotherms using the Barrett–Joyner–Halenda (BJH) method [19]. The adsorption branch was favored over the desorption branch in order to avoid the tensile strength effect (TSE) artifact which very often complicates the PSD determination in mesoporous systems [20].

Derivatograph Q thermobalance, MOM Hungary, was used for investigation of thermal behavior of the

specimens. About 100 mg of samples were placed in the ceramic crucible sample holder. The temperature was ramped by 10 degree/min from ambient to 1300 K in air.

The removal of organic compounds used for the synthesis of both the silicate and the platinum nanoparticles was checked by IR spectroscopy (Mattson, Genesis FTIR spectrometer). 1 mg of sample was homogenized in 200 mg KBr (spectroscopic grade) and pressed to a disc shape wafer. The spectra of samples were recorded against KBr.

2.4. In situ IR spectroscopic measurements

For *in situ* IR measurements self-supported wafer was pressed from the samples and placed into the IR cell followed by heat treatment at 500 °C in flowing oxygen for 2 h. Then it was cooled to 573 K and reductive treatment was performed in hydrogen for 1 h *in situ* in the IR cell. After evacuation the sample was cooled to ambient temperature and the spectrum of the wafer was registered.

After activating the wafer and registering the baselines of both the wafer and the empty IR cell, the vacuum line allowed us to load the wafer with different gases and treat the sample in various atmospheres including vacuum at different temperatures. For the hydrogenation experiments the cell was loaded with cyclohexene:hydrogen mixtures of 1:1, 1:3, 1:5 and 1:10 molar ratios. Both the gas phase and the adsorbed phase spectra were recorded with reaction time. The adsorbed phase and the gas phase were investigated by placing the catalyst wafer in and out of the light path, respectively. From these spectra we obtained information on the products formation and on the surface intermediate generation at given temperatures. This IR reactor cell system was considered as a static, not stirred tank reactor with a volume of 500 ml. The total initial pressure of the reactants in the system was 110 Torr. The initial rate was determined from the reactant concentration versus reaction time curves by graphic interpolation. All catalytic tests were repeated three times to assure reproducibility. Preliminary experiments indicated that no diffusion limitations were present within the range of operating conditions.

3. Results and discussion

3.1. Preparation and pretreatment of the catalysts

Figure 1 shows the TEM images of platinum nanoparticles prepared by the different surface protecting agents. Figure 1A shows the case when no surface protecting agent was used for the synthesis of the Pt nanoparticles. The histogram reveals a rather broad particle size distribution (7.2 ± 2.8 nm). For particles shown in part figure 1B NIPA was used as capping agent. As the histogram shows the particle size distribution is narrow (3.6 ± 0.67 nm) and the most part of the particles has cubic shape (in details see ref. [4]). In figure 1C the TEM image of the particles shows their tetrahedral shape and their rather uniform (3.2 ± 0.64 nm) size. In this case PVP was used as surface protecting agent.

3.2. Mechanical stability of SBA-15 support and Pt/SBA-15 catalysts

The parent sample of SBA-15 was synthesized adopting the description found in the literature. The XRD profile of the sample showed a well ordered structure. It had a BET surface area of 738 m^2/g and an average pore size of 6.5 nm. In the TEM image (figure 2) both the parallel channels and the hexagonal arrangement of channels could be recognized.

In figure 3 the two TEM images show the difference between the samples prepared by impregnation and sonication aided impregnation. The impregnation with colloid solution Pt nanoparticles synthesized in the absence of surface protecting agent leads to a catalyst having platinum nanoparticles on the outer surfaces of the mesoporous support (figure 3A). This finding has been expected since the size of most of these particles was too big to get into the channels of the SBA-15. Contrary to this, the sonication aided impregnation results in samples containing platinum nanoparticles mostly interior the pore system (figure 3B).

In order to check the application of SBA-15 silicates as catalyst support for platinum nanoparticles we investigated the resistance of this mesoporous material against the pressure. It seemed to be obligatory since in a part of the characterization methods pressed wafers or pellets are used. Figure 4 shows the SAXS patterns of SBA-15 samples pressed into disc shape wafers using different pressures. It is seen that reflection due to the pore openings (or d_{100}) gradually decreases with increasing pressures. Above 50 bar the intensity is less than half of the original.

We measured the nitrogen adsorption isotherms at 77 K. The measured values are depicted in figure 5A. There are two recognizable features.

The first is the moderate decrease of the BET surface areas (see in table 1) and a parallel substantial decrease the volume of nitrogen adsorbed close to the relative pressure 1. The pore size distribution curves exhibited in figure 5B show the formation of bimodal pore system with increasing palletizing pressure. The portion of characteristic pore size around 5 nm decreasing and simultaneously smaller pores centered around 3.5 nm developed. After 100 bar pressure exclusively such small pores are present in the sample. From these results we concluded that using a pressure around 5 bar is recommended to press wafers or discs for any

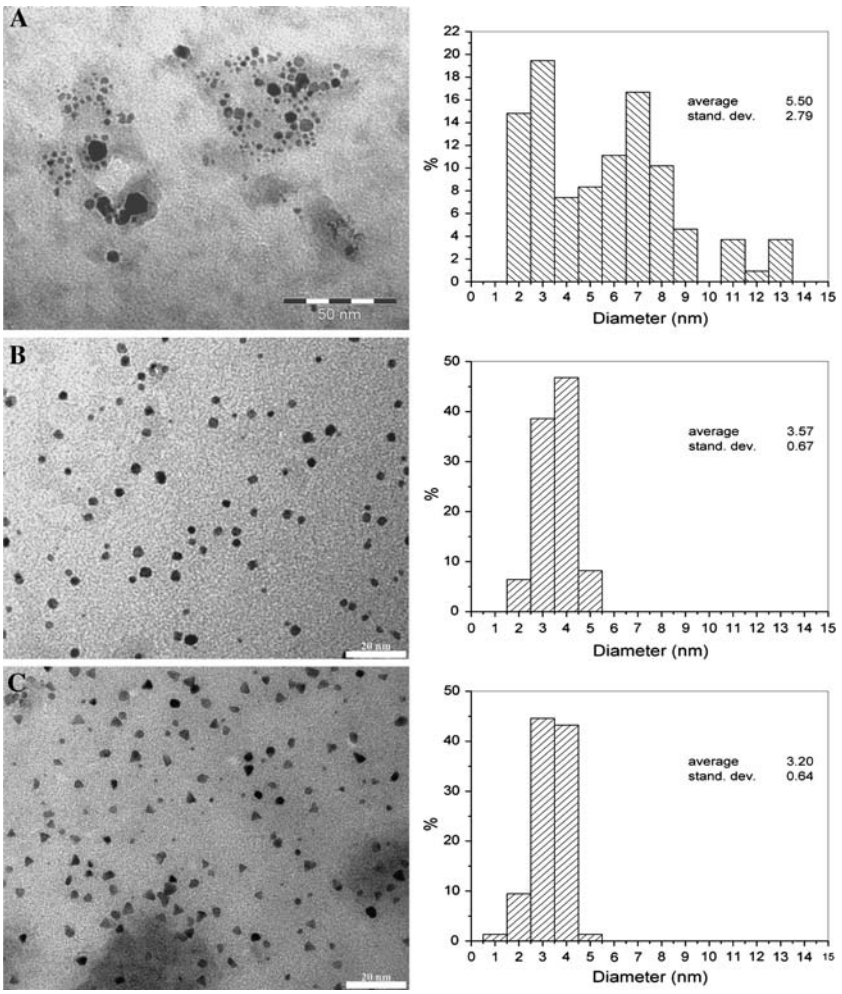

Figure 1. Preparation of Pt nanoparticles (A) without surface protecting agent, (B) with NIPA, and (C) with PVP as a capping agent.

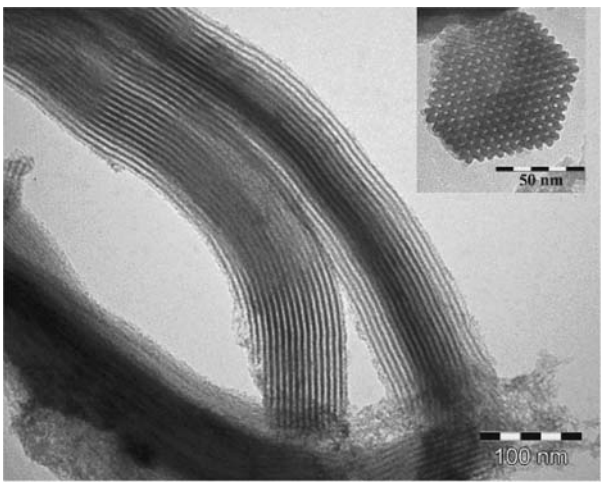

Figure 2. TEM images of the calcined SBA-15.

characterization procedures and also for catalytic runs. This finding is in accordance with those reported by Borodko *et al*. [21].

3.3. Thermal stability of SBA-15

As the next parameter the temperature of pretreatment was investigated. In catalysis the catalyst samples are subjected to different heat treatment in various atmospheres preceding the catalytic reaction. It is indispensable to know the thermal stability of the catalyst including the catalyst support itself. As the mesoporous silicates are synthesized in the presence of organic templates filling the pores in the as synthesized material, an appropriate heat treatment in air or oxygen is generally used to burn these template molecules off. In some cases the burning results in the partial collapse of the ordered structure. For these, temperature sensitive derivatives some other procedures are offered to get ride of organics from the mesopores. The TG–DTG measurements showed that samples heat treated at 600 °C preserves their ordered structure. This finding was supplemented by the BET measurements. Up to 700 °C only a slight decrease was observed. These small differences in the values can be regarded as deviation of the measurements. As seen in figure 6 the shape of the

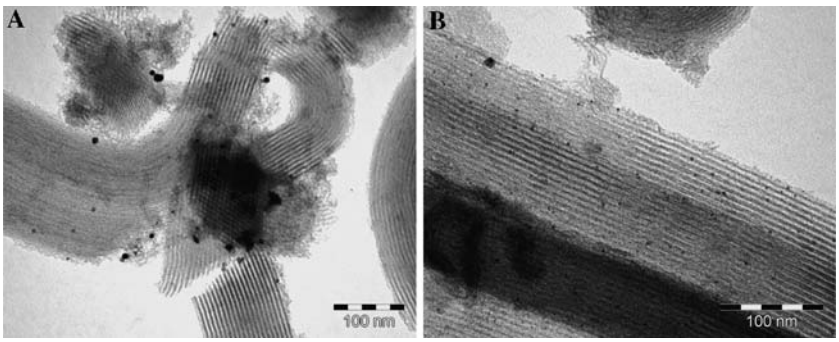

Figure 3. TEM images of the SBA-15 samples prepared with (A) impregnation of colloidal solution of large nanoparticles, and (B) ultrasonic aided impregnation.

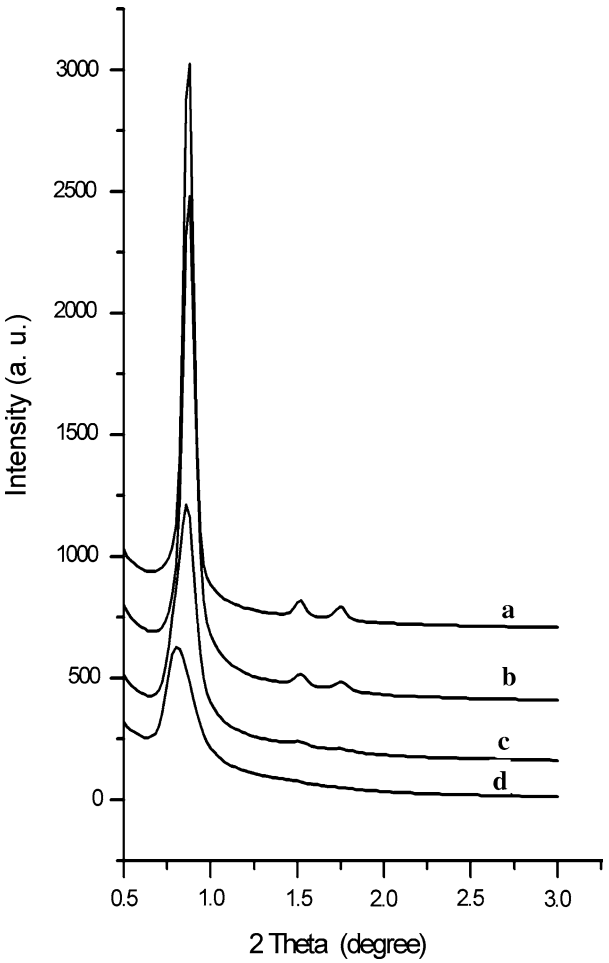

Figure 4. SAXS patterns of SBA-15 using different pressure at pelleting: (a) SBA-15, (b) 5 bar, (c) 50 bar, (d) 100 bar.

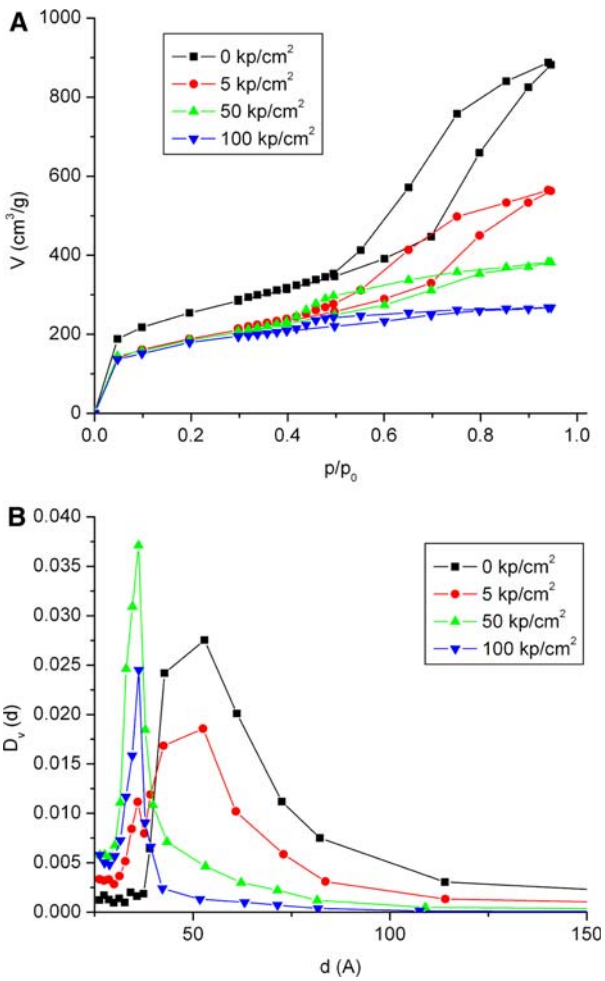

Figure 5. Nitrogen adsorption–desorption isotherms (A) and pore size distribution (B) of SBA-15 using different pelleting pressure.

nitrogen adsorption isotherms is very similar; the specific surface area values only slightly decreased. A significant change has been obtained only after treatment at 900 °C. The treatment at 900 °C resulted in significant decrease in the specific surface area (455 m^2/g). From these results we concluded that the burning of template can be performed up to 600 °C and we used this procedure in our practice.

3.4. *The influence of sonication on the preparation of catalysts*

The impregnation is a conventional preparation method for production of supported metal catalysts. The procedures, both the incipient wetness and the classical impregnation, did not destroy the support if it is resistant against the solvent used. When we use

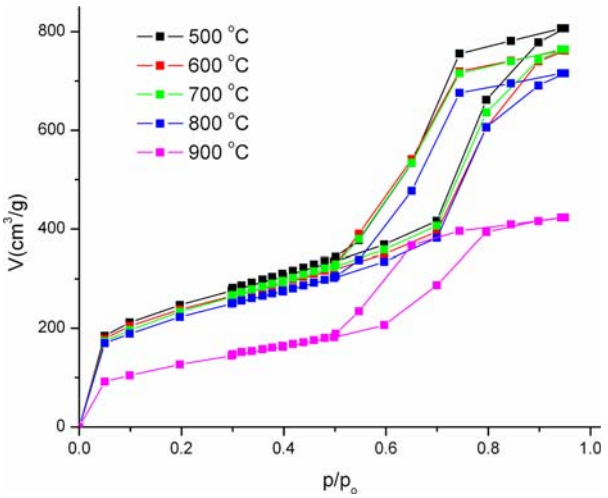

Figure 6. Nitrogen adsorption–desorption isotherms of SBA-15 after calcination at different temperatures.

Table 1
Specific surface area of SBA-15 using different pelleting pressure

Applied pressure	Specific surface area (m^2/g)
0 bar	738
5 bar	656
50 bar	636
100 bar	605

sonication for better distribution of the metal particles or to introduce the particles into the pores some moderate destruction of the support may be expected. Depending on the efficiency of sonication this destruction may become drastic. In our laboratory a low energy ultrasonic bath is used for catalyst preparation. Contrary to this we checked the influence of it on the structural features of SBA-15 support. As the BET data in table 2 show the concentration of platinum particles introduced into the SBA-15 pores influences the BET values. The higher the concentration the lower is the BET value. The explanation of this feature can be as follows. With increasing the number of particles entering the pores the pore volume decreases (this can be seen in the nitrogen adsorption–desorption isotherms in figure 7).

Table 2
Specific surface area of different platinum containing SBA-15 before and after the 2nd calcination

Concentration (wt%)	Specific surface area (m^2/g)	
	Before calcination	After calcination
SBA-15	738	–
0.01% Pt	675	656
0.05% Pt	647	644
0.10% Pt	532	553
0.50% Pt	548	564
1.00% Pt	361	290

Note that after finishing the treatment in the ultrasonic bath the samples were transferred into the Rotavap system and the solvent was evaporated. The dry material was used as catalyst precursor. During this procedure not only the platinum particles but also the respective surface protecting agents has been introduced into the pores. This is the reason why the catalyst precursor has to be heat treated again (so-called 2nd calcination). Since the interaction between the surface protecting compound and the platinum nanoparticles is quite strong, to remove this organic matter burning seemed to be the most convenient way. This oxidative treatment was performed at 500 °C resulting in a spectroscopically clean surface (no CH bands can be observed). We believe that despite this quite strong treatment the platinum nanoparticles can resolve their size and shape, since it was shown that on silica support the platinum nanoparticles are quite stable below 500 °C due to the interfacial mixing of Pt and SiO_2 and the resulting negative interface energy [22].

Comparing the BET values before and after the 2nd calcination step (see table 2) no significant change was observed, thus the structure destroying effect of this treatment can be neglected.

The next question is the following: how big pore volume is occupied by these moieties in the pores? We found that it is significant as the values of nitrogen adsorption data show (figure 7). From these results we can conclude that the decrease of BET area with increasing the concentration of platinum nanoparticles is partly due to the diminished room available for adsorbed nitrogen. An additional factor cannot be neglected as well. This is the mechanical breaking of the ordered straight pores by the platinum nanoparticles arriving to the pore opening or arriving to the surrounding of the pores. As we found such a process may contribute to the decrease of the BET values.

3.5. *Template removal, surface cleaning procedures*

When we start with the reaction kinetic measurement we should have an organic free catalyst. In two stages of the preparation procedure we have to remove organic compounds from the samples, firstly the organic templates filling the pores of the "as synthesized" oxide support material, and in the second step the nanoparticle surface protecting compound we introduced into the sample upon loading the platinum nanoparticles. Firstly, we discuss the template removal. For this purpose we investigated some other procedures besides the burning the organic molecules off. As can be seen in the IR spectra displayed in figure 8 neither a simple evacuation of the silicate at 450 °C for 2 h nor leaching the "as synthesized" SBA-15 in ethanol for several hours resulted in organic free material. The group of bands

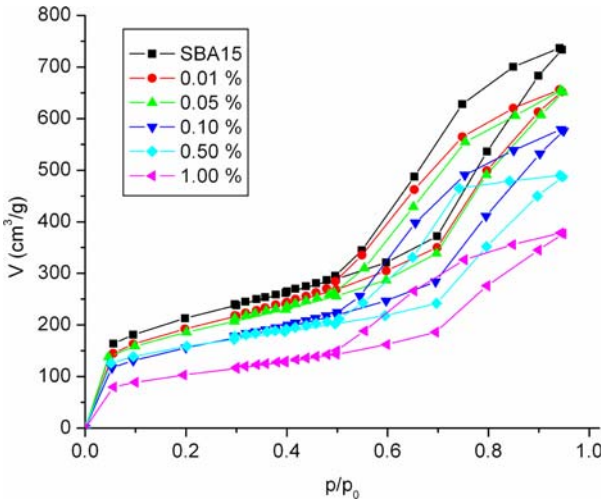

Figure 7. Nitrogen adsorption–desorption isotherms of SBA-15 with different platinum content.

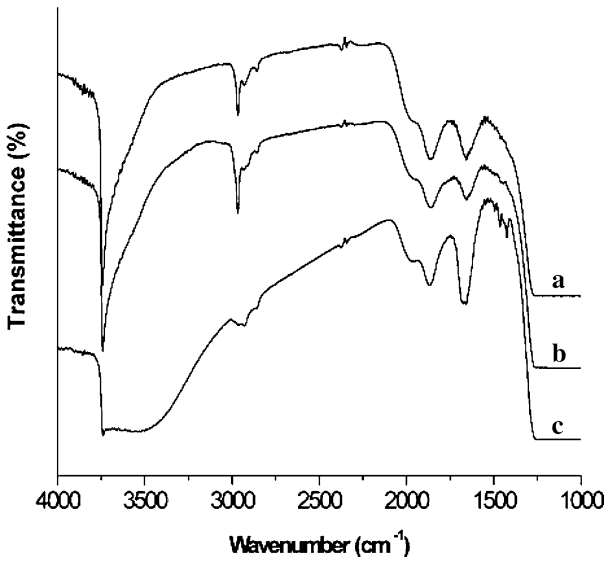

Figure 8. IR spectra of SBA-15 containing 0.1 wt% Pt (PVP, impr.) The surface cleaning procedure was: vacuum at 450 °C (a), reflux in ethanol (b), oxidation with hydrogen peroxide (c).

around 2900 cm^{-1} characteristic of the methyl- and methylene-groups of organic residues could be observed after these treatments. The oxidation with hydrogen peroxide in aqueous solution proved to be ineffective as well. The only procedure gave organic free sample at this stage of preparation was the burning in air at 550 °C. Neither this nor the treatment at 600 °C, did not cause any detectable structural change, as we discussed before. For all the platinum particles containing samples, the SBA-15 support was treated in this way preceding the sonication aided impregnation process.

3.6. Catalytic features of nanoparticles

We have tested several catalysts in the hydrogenation of cyclohexene. About choosing this reaction we have described briefly in the introduction. In previous papers we indicated that differences can be found in the catalytic behavior of catalysts samples loaded by tetrahedral or cubic platinum nanoparticles [5]. We have observed that the catalytic performance of the samples produced by loading the support with platinum nanoparticles is very sensitive to the reaction temperature. This feature can be attributed to the increased surface energies of metal nanoparticles present in quite uniform size distribution and shape in the catalyst support. Further experiments are in progress to collect more information to this point. For this purpose a new IR cell is designed allowing measurements in wide temperature range including below room temperature that is the lower limit of our present system. The catalyst having 0.1% cubic shape Pt nanoparticles possesses rather high activity even at room temperature since 100% conversion was observed around 90 min in the hydrogenation of cyclohexene. Above 100 °C the rate of the reaction was fast approaching the upper limit of the measurement. Therefore the influence of platinum loading and the cyclohexene/hydrogen ratio has been investigated at ambient temperature.

3.7. Influence of the concentration of platinum nanoparticle on SBA-15 support

Figure 9 shows the formation of cyclohexane in the hydrogenation of cyclohexene over catalysts containing increasing amount of platinum nanoparticles. The kinetic curves were measured under identical experimental conditions indicated in the figure captions. The lowest catalytic activity was found for sample possessing

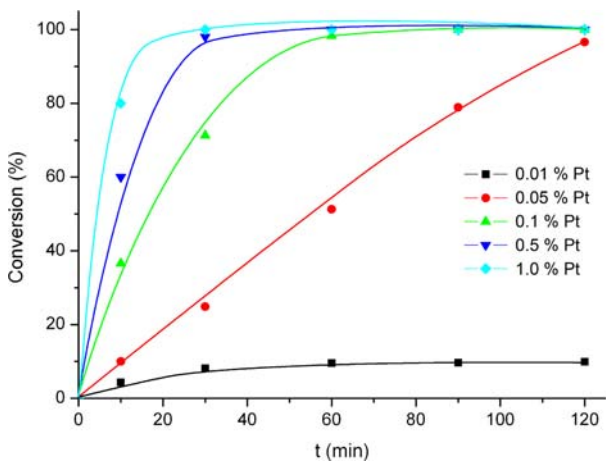

Figure 9. Kinetic curves of cyclohexene hydrogenation over Pt/SBA-15 catalysts having different metal loadings ($T_{reaction}$ = 25 °C, $p_{Hydrogen}$ = 10 Torr, $p_{Cyclohexene}$ = 100 Torr.)

Table 3
Initial rates of hydrogenation reaction of cyclohexene on different platinum containing SBA-15 catalysts

Pt concentration (wt%)	Initial rate (mol/s)
0.01% Pt	1.541×10^{-6}
0.05% Pt	4.454×10^{-6}
0.10% Pt	1.804×10^{-5}
0.50% Pt	3.016×10^{-5}
1.00% Pt	5.145×10^{-5}

0.01% Pt. The shape of this curve shows a saturation character indicating no further transformation suggesting deactivation of the metal after very short reaction time. With increasing platinum loading the rate increases as it can be seen in table 3.

3.8. *Influence of the cyclohexene/hydrogen ratio on the reaction rate on tetrahedral and cubic particles*

Figure 10 shows the formation of cyclohexane in reactions of hydrogenation using different cyclohexene/hydrogen ratios over cubic and tetrahedral platinum nanoparticles supported on SBA-15 silicate, whereas table 4 shows the calculated initial rates. Strong influence of the hydrogen pressure was observed for both catalysts. The kinetic curves for cyclohexene/hydrogen = 1 molar ratio run to saturation, indicating the deactivation of the catalysts under these conditions. Reaction mixtures containing more hydrogen show much better catalytic performances. At cyclohexene/hydrogen = 10 ratio, the difference in the shape of the cyclohexane production curve suggest that the reaction is faster over platinum particles of tetrahedral morphology. This finding is in complete agreement with those reported by Somorjai and McCrea on single crystal surfaces [23]. In the cited paper, figure 1 shows the turnover rates for hydrogenation of cyclohexene using 10 Torr of substrate and 100 Torr of hydrogen identical to our experiment. The initial part of the maximum curves has larges slope for the reaction due to the Pt (111) surface. The authors concluded that the maximum of the turnover rate of hydrogenation appeared at lower temperature than the dehydrogenation and the maximum for hydrogenation was higher on

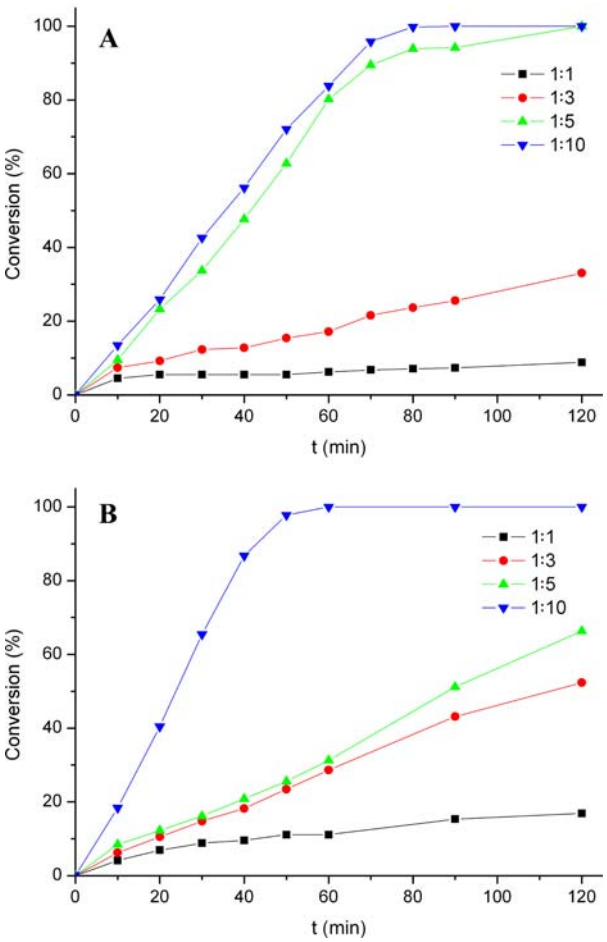

Figure 10. Kinetic curves of cyclohexene hydrogenation using different cyclohexene/hydrogen ratios over Pt/SBA-15 catalysts containing cubic (A) and tetrahedral (B) platinum nanoparticles prepared by using NIPA and PVP as surface protecting agents, respectively. ($T_{reaction}$ = 25 °C, $p_{Cyclohexene}$ = 100 Torr.)

Table 4
Initial rates of cyclohexene hydrogenation using different cyclohexene/hydrogen ratios over Pt/SBA-15 catalysts containing cubic (A) and tetrahedral (B) platinum nanoparticles

Cyclohexene/H_2 ratio	A Initial rate (mol/s)	B Initial rate (mol/s)
1:1	2.089×10^{-6}	1.817×10^{-6}
1:3	3.274×10^{-6}	2.726×10^{-6}
1:5	4.361×10^{-6}	3.817×10^{-6}
1:10	6.009×10^{-6}	8.183×10^{-6}

Pt (111) while lower on Pt (100) faces than that of the dehydrogenation. The phenomenon was traced back to the difference of reaction mechanisms on the two different surfaces. This finding may serve as an excellent test reaction occurring with different rates over different crystal faces. Our aim was to show if this phenomena can be observed on platinum nanoparticles or not.

3.9. Comparison of structural and catalytic behavior of macroscopic and nanosized crystal facets

Investigations of the catalytic behavior of single crystal facets gave several important conclusions for the researchers working with supported metal catalysts. The randomly distribution of various crystal faces, being present particularly at the edges, corners, kinks and terraces of the metal component results in an averaged activity and selectivity in any reactions. The most promising way to enhance the selectivity of a supported catalyst was to modify the ratio of different crystal faces. However, it seems to be a hard task, to decrease the portion of a given crystal face at the expense of another. To achieve such a goal the knowledge on influence of each possible crystal face is indispensable. These data can be obtained by investigating the catalytic characteristics of single crystal faces in separate experiments. To adopt these results to supported metal catalysts prepared by the conventional methods, i.e. by impregnation of the support by metal salt solution followed by decomposition of the salt and reduction of the metal ion to metal is not easy and may lead misinterpretation of the observed results. At present we think that impregnation of the support by platinum nanoparticles prepared in separate experiments might give better, intermediate resolution for modeling a catalyst between the single crystals and supported metals having nanosized metal particles. When metal particles can be synthesized with different morphologies, such as tetrahedral and cubic available for platinum, varying their ratio on the support catalysts of predetermined characteristics can be obtained. A detailed kinetic study of such catalyst series may give more and basic information on the contribution of different facets to the catalytic performance. However this approximation might have some weak points as well. The origin of these is on one side the increased surface energies of the nanocrystals that may decrease the activation energy or increase the surface reconstruction drastically. On the other side the relative low stability of the nanoparticles that may result in fast agglomeration and generation of oversized metal particles. The later feature can be slow down by incorporation of metal nanoparticles into porous matrices. We have given an example to this point in the current paper. The control of the former features is much harder work. As we reported for the platinum nanocrystals the temperature dependence of the investigated reaction was rather strong. A reasonable solution would be to make experiments in much lower temperatures. These kinds of measurements are in progress in our laboratories.

4. Conclusions

Platinum nanoparticles with different shapes were prepared and used for preparation of supported metal catalysts. For supporting the platinum particles SBA-15 mesoporous silicate was used because it has a quite large specific surface area and ordered pore system.

For the production of supported platinum catalysts sonication assisted impregnation of SBA-15 silicate was utilized and investigated in details. We have shown that the platinum nanoparticles dominantly are interior the pores. The stability of the samples proved to be high, probably due to the shadowing property of the pore interior, allowing a quite severe pretreatment for the removal of the surface protecting compounds.

We have tested several pretreatment conditions in order to remove the organic matter from the catalyst particles. A two-step activation procedure, in which the first step is an oxidative treatment at 500 °C, ending by an evacuation at 300 °C was found to be appropriate.

We optimized the formulation of the synthesized samples. We showed that the pressure used for preparation of self-supported wafers should not be exceeded the 5 MPa, since at higher pressure partial collapse of the ordered mesostructure takes place. This finding was concluded from BET and XRD experiments.

We showed that IR spectroscopy is a fruitful tool for investigation of catalytic behavior of SBA-15 supported catalysts when the platinum loading is low since the SBA-15 mesoporous silicate is inactive in the transformation of cyclohexene and its hydrogenated or dehydrogenated derivatives. Simultaneous analysis of the spectra of the wafer and the surrounded gas phase allowed following the changes both in the adsorbed and in the gas phase.

The reaction temperature plays the determining role in the hydrogenation. The reaction was so fast above 100 °C that the product analysis became uncertain. The system we used allowed decreasing the reaction temperature to ambient. Between these limits we measured the reaction rate which followed the usual kinetic

picture. As far as the catalyst containing platinum particles of almost identical size but different morphology is concerned, the above mentioned feature has been supplemented. This very high sensitivity towards the reaction temperature can be traced back to the high surface energy of platinum nanoparticles.

Investigations on the influence of hydrogen/cyclohexene molar ratio showed that the higher this ratio the faster the reaction rate is.

Following a recent paper of Somorjai et al. in which they proved that the rate of cyclohexene hydrogenation is influenced by the symmetry of the platinum single crystal faces [23], our aim was to investigate if this phenomena can be observed on supported platinum nanoparticles or not. Somorjai et al. concluded that the maximum rate for hydrogenation was higher on Pt (111) while lower on Pt (100) faces. The phenomenon was traced back to the difference of reaction mechanisms on the two different surfaces. Our results, namely the reaction rates over catalysts containing either tetrahedral (PVP capped particles) or cubic (NIPA capped particles) platinum nanoparticles in identical concentration in a reacting mixture consisting of 10 Torr cyclohexene and 100 Torr hydrogen showed excellent agreement with those obtained for 100 and 111 Pt single crystals [23].

Acknowledgment

Authors thank the Hungarian Academy of Sciences and the National Science Foundation for the financial support the project (DMR-0244146). ZK acknowledges the financial support of the MTA Bolyai Janos Research Fellowship.

References

[1] G.C. Bond, *Heterogeneous Catalysis: Principles and Applications* (Oxford University Press, 1987).
[2] G.A. Somorjai, Catal. Lett. 9 (1991) 311.
[3] Z. Kónya, V.F. Puntes, I. Kiricsi, J. Zhu, J.W. Ager, M.K. Ko, H. Frei, A.P. Alivisatos and G.A. Somorjai, Chem. Mater. 15 (2003) 1242.
[4] Z. Kónya, V.F. Puntes, I. Kiricsi, J. Zhu, A.P. Alivisatos and G.A. Somorjai, Nano Lett. 2 (2002) 907.
[5] Z. Kónya, V.F. Puntes, I. Kiricsi, J. Zhu, A.P. Alivisatos and G.A. Somorjai, *Catal. Lett*. 81 (2002) 137; E. Molnar, G. Tasi, Z. Konya, I. Kiricsi, *Catal. Lett*. 101 (2005) 159.
[6] R. Yu, H. Song, X.-F. Zhang and P. Yang, J. Phys. Chem. B 109 (2005) 6940.
[7] V.Y. Gusev, X. Feng, Z. Bu, G.L. Haller and J.A. O'Brien, J. Phys. Chem. 100 (1996) 1985.
[8] T. Ishikawa, M. Matsuda, A. Yasukawa, K. Kandori, S. Inagaki, T. Fukushima and S. Kondo, J. Chem. Soc. Faraday Trans. 92 (1996) 1985.
[9] S.B. McCullen, J.C. Vartuli, Mobil Oil Corporation, US Patent 5/156829 (1992).
[10] M. Hartmann and C. Bischof, J. Phys. Chem. B 103 (1999) 6230.
[11] T. Tatsumi, K.A. Koyano, Y. Tanaka and S. Nakata, Chem. Lett. 5 (1997) 469.
[12] K.A. Koyano, T. Tatsumi, Y. Tanaka and S. Nakata, J. Phys. Chem. 101 (1997) 9436.
[13] A. Fudala, I. Kiricsi, S.I. Niwa, M. Toba, Y. Kiyozumi and F. Mizukami, Appl. Catal. A: Gen. 176 (1999) L153.
[14] A. Miyazaki, I. Balint and Y.J. Nakano, Nanopart. Res. 5 (2003) 69.
[15] J.L. Elechiguerra, L. Larios-Lopez and M. Jose-Yacaman, Appl. Phys. A 84 (2006) 11.
[16] I. Balint, A. Miyazaki and K. Aika, Appl. Catal. B. 37 (2002) 217.
[17] J. Zhu, Z. Konya, V.F. Puntes, I. Kiricsi, C.X. Miao, J.W. Ager, A.P Alivisatos and G.A. Somorjai, Langmuir 19 (2003) 4396.
[18] M.S. Morey, S. O'Brien, S. Schwarz and G.D. Stucky, Chem. Mater. 12 (2000) 898.
[19] E.P. Barrett, L.G. Joyner and P.P. Halenda, J. Am. Chem. Soc. 73 (1951) 373.
[20] J.C. Groen, L.A.A. Peffer and J. Perez-Ramırez, Micropor. Mesopor. Mater. 60 (2003) 1.
[21] Y. Borodko, J.W. Ager, G.E. Marti, H. Song, K. Niesz and G.A. Somorjai, J. Phys. Chem. B. 109 (2005) 17386.
[22] R. Yu, H. Song, X.-F. Zhang and P. Yang, J. Phys. Chem. B. 109 (2005) 6940.
[23] K.R. McCrea and G.A. Somorjai, J. Mol. Catal. A: Chem. 163 (2000) 43.